Heterobimetallic Complexes Based on $[(Tp)Fe(CN)_3]^-$: Syntheses, Crystal Structures and Magnetic Properties

Shi Wang,[a] Jing-Lin Zuo,*[a] Hong-Cai Zhou,[b] You Song,[a] Song Gao,[c] and Xiao-Zeng You*[a]

Keywords: Chain structures / Cyanide ligands / Iron / Magnetic properties / Polynuclear complexes

With the anionic precursor $[(Tp)Fe^{III}(CN)_3]^-$ [**1**; Tp: hydrotris(pyrazolyl)borate] as a building block, two trinuclear complexes, $[(Tp)_2Fe^{III}{}_2(CN)_6Mn(CH_3OH)_4]\cdot 2CH_3OH$ (**2**), $[(Tp)_2Fe^{III}{}_2(CN)_6Ni(cyclam)]\cdot 2H_2O$ (**3**; cyclam: 1,4,8,11-tetraazacyclotetradecane) and a one-dimensional polymer, $[(Tp)Fe^{III}(CN)_3Cu(dien)]ClO_4\cdot H_2O$ (**4**; dien: diethylenetriamine), have been synthesized and structurally characterized. In complex **2**, each of the two $[(Tp)Fe(CN)_3]^-$ units binds through one of its three cyanide groups to a central $[Mn(CH_3OH)_4]^{2+}$ core. In complex **4**, a zigzag chain is formed by combining $[TpFe(CN)_3]^-$ and $[Cu(dien)]^{2+}$ fragments alternately through cyano bridges. The magnetic properties of complexes **2**–**4** have been investigated in the temperature range 2–300 K. A weak antiferromagnetic interaction between the Mn^{II} and Fe^{III} ions has been found in complex **2**. The magnetic data of **2** can be fitted with the isotropic Hamiltonian $\hat{H} = -2J(\hat{S}_1\cdot\hat{S}_2 + \hat{S}_2\cdot\hat{S}_3) - 2J'\hat{S}_1\cdot\hat{S}_3$, where J and J' are the intramolecular exchange coupling parameters between adjacent and peripheral spin carriers, respectively. This leads to values of $J = -2.19$ cm^{-1} and $g = 2.13$. The same fitting method was applied to complex **3** to give values of $J = 17.2$ cm^{-1} and $g = 2.37$, showing that there is a ferromagnetic interaction between the Fe^{III} and Ni^{II} ions. The 1-D chain of **4** is treated as alternating uniform Fe–Cu dimers with different intradimeric (J_d) and interdimeric (J_c) exchange constants, leading to $J_d = 10.9$ cm^{-1}, $J_c = 1.29$ cm^{-1} and $g = 2.54$.

Introduction

Tremendous effort has been devoted to the study of cyanide-containing metal complexes because of their unique magnetic properties, such as high-*Tc* magnetism and light- or pressure-tuning of magnetization.[1−4] Among those, low-dimensional as well as polynuclear clusters have attracted much attention since such systems can be used to investigate the intermetallic magnetic coupling quantitatively; there is no appropriate model for quantitative magnetic analysis to high-dimenisonal systems. Recently, synthetic strategies to prepare cyanide-bridged bimetallic systems by using modified cyanometalates as multidentate ligands and linkers have been developed. The following are representative examples: $[(tacn)M(CN)_3]$ ($M = Co^{3+}$, Cr^{3+}; tacn = 1,4,7-triazacyclononane),[5] $[(Me_3tacn)M(CN)_3]$ ($M = Cr^{3+}$, Mo^{3+}; Me_3tacn = *N*,*N*′,*N*′′-trimethyl-1,4,7-triazacyclononane),[6] $[(tach)M(CN)_3]$ ($M = Cr^{3+}$, Fe^{3+}, Co^{3+}; tach = 1,3,5-triaminocyclohexane),[7] $[Fe(bipy)(CN)_4]^-$, $[Fe(bipy)(CN)_4]^{2-}$ and $[Fe(phen)(CN)_4]^-$ (bipy = 2,2′-bipyridine; phen = 1,10-phenanthroline).[8,9] In an effort to extend this interesting chemistry, we chose the tailored cyanometalate precursor $(Bu_4N)[(Tp)Fe(CN)_3]$ [**1**; Tp = hydrotris(pyrazolyl)borate; Bu_4N^+ = tetrabutylammonium cation], which consists of three CN^- groups and a hydrotris(pyrazolyl)borate (Tp) ligand. The anion has recently been reported by Julve's group as its tetraphenylphosphonium salt.[10] Tp is a classical scorpionate ligand containing a C_3 axis. It has been used as a protecting group to prepare topological analogues of the P clusters of nitrogenase.[11] Compared to tacn-type ligands, Tp is sterically similar but bears a negative charge. Thus, it may direct the formation of new complexes with interesting structures and magnetic properties. Herein, we report the preparation, crystal structures and magnetic properties of two trinuclear complexes $[(Tp)_2Fe^{III}{}_2(CN)_6Mn(CH_3OH)_4]\cdot 2CH_3OH$ (**2**) and $[(Tp)_2Fe^{III}{}_2(CN)_6Ni(cyclam)]\cdot 2H_2O$ (**3**; cyclam: 1,4,8,11-tetraazacyclotetradecane), and a one-dimensional polymer $[(Tp)Fe^{III}(CN)_3Cu(dien)]ClO_4\cdot H_2O$ (**4**; dien: diethylenetriamine).

[a] Coordination Chemistry Institute, State Key Laboratory of Coordination Chemistry, Nanjing University, Nanjing 210093, China
[b] Department of Chemistry and Biochemistry, Miami University, Oxford, OH 45056-1465, USA
[c] State Key Laboratory of Rare Earth Materials Chemistry and Applications, College of Chemistry and Molecular Engineering, Peking University, Beijing 100871, China

Results and Discussion

Synthesis and Spectral Features

In this paper the anionic precursor $[(Tp)Fe(CN)_3]^-$ (**1**) is used as a building block to prepare cyanide-bridged multinuclear clusters and coordination polymers. The tetrabutylammonium salt of **1** was isolated as an orange crystalline solid in 78% yield. Only one C≡N stretching vibration (2117 cm^{-1}) is observed in its IR spectrum. It is soluble in most organic solvents such as acetonitrile, acetone, methanol and DMF.

Reaction of $Mn(ClO_4)_2$ with $(Bu_4N)[(Tp)Fe^{III}(CN)_3]$ (**1**) in methanol yields the trinuclear complex $[(Tp)_2Fe^{III}{}_2(CN)_6Mn(CH_3OH)_4]\cdot 2CH_3OH$ (**2**). The occurrence of two peaks of medium intensity in the C≡N stretching region of the IR spectrum is consistent with the presence of bridging (2151 cm^{-1}) and terminal (2129 cm^{-1}) cyanide ligands. Another trinuclear complex, $[(Tp)_2Fe^{III}{}_2(CN)_6Ni(cyclam)]\cdot 2H_2O$ (**3**), was formed from the reaction of $Ni(cyclam)(ClO_4)_2$ and $(Bu_4N)[(Tp)Fe(CN)_3]$ in ethanol and water. The C≡N stretching frequencies are located at 2119 and 2157 cm^{-1}. Both complexes are soluble in some organic solvents. The solvates in both **2** and **3** can easily lose solvent upon exposure to air.

The reaction of $Cu(ClO_4)_2\cdot 6H_2O$, dien and $(Bu_4N)[(Tp)Fe(CN)_3]$ in aqueous solution leads to the formation of brown, crystalline $[(Tp)Fe^{III}(CN)_3Cu(dien)]ClO_4\cdot H_2O$ (**4**). The C≡N stretching region of the IR spectrum of **4** is consistent with the presence of bridging (a peak of medium intensity at 2157 cm^{-1}) and terminal (a weak absorption at 2131 cm^{-1}) cyanide ligands.

Crystal Structures

Selected bond lengths and angles for complexes **2**−**4** are compiled in Table 1−3.

Table 1. Selected bond lengths and angles in complex **2**

Bond lengths (Å)			
Fe(1)−N(2)	1.975(2)	Fe(1)−N(4)	1.966(2)
Fe(1)−N(6)	1.977(3)	Fe(1)−C(10)	1.931(3)
Fe(1)−C(11)	1.928(3)	Fe(1)−C(12)	1.915(3)
C(12)−N(9)	1.149(4)	Mn(1)−N(9)	2.174(2)
Mn(1)−O(1)	2.198(2)	Mn(1)−O(2)	2.1906(19)
Bond angles (°)			
Fe(1)−C(10)−N(7)	177.9(3)	Fe(1)−C(11)−N(8)	175.9(3)
Fe(1)−C(12)−N(9)	176.1(3)	Mn(1)−N(9)- C(12)	167.2(2)
C(11)−Fe(1)−C(12)	86.98(13)	C(10)−Fe(1)−C(12)	87.06(12)
N(9)−Mn(1)−O(1)	89.72(9)	N(9)−Mn(1)−O(2)	90.63(8)

The ORTEP drawing for complex **2** is depicted in Figure 1. Complex **2** consists of a trinuclear $[\{(Tp)Fe(CN)_3\}_2Mn(CH_3OH)_4]$ cluster and two methanol solvate molecules. In this trinuclear cluster, the $[(Tp)Fe(CN)_3]^-$ unit acts as a monodentate ligand through one of its three cyanide groups toward a central $[Mn(CH_3OH)_4]^{2+}$ core. Each iron(III) ion is coordinated by three Tp nitrogen atoms and three cyanide carbon atoms, with a C_{3v} symmetry. The Fe(1)−C(cyano) bond lengths [1.915(3)−1.931(3) Å] are in good agreement with those observed in other low-spin iron(III) complexes.[8,9] The Fe−C≡N angles for both terminal [175.9(3)° and 177.9(3)°] and bridging [176.1(3)°] cyanide groups depart slightly from strict linearity. The manganese atom is six-coordinate in a

Table 2. Selected bond lengths and angles in complex **3**

Bond lengths (Å)			
Fe(1)−C(11)	1.928(4)	Fe(1)−C(12)	1.911(4)
Fe(1)−C(10)	1.938(4)	Fe(1)−N(4)	1.978(3)
Fe(1)−N(6)	1.989(3)	Fe(1)−N(2)	1.997(3)
C(11)−N(8)	1.144(5)	C(10)−N(7)	1.132(5)
C(12)−N(9)	1.143(5)	Ni(1)−N(9)	2.096(3)
Ni(1)−N(10)	2.052(3)	Ni(1)−N(11)	2.070(3)
Bond angles (°)			
Fe(1)−C(11)−N(8)	179.0(4)	Fe(1)−C(10)−N(7)	178.6(4)
Fe(1)−C(12)−N(9)	177.8(4)	Ni(1)−N(9)−C(12)	171.5(3)
C(11)−Fe(1)−C(12)	84.97(16)	C(10)−Fe(1)−C(12)	89.21(16)
N(9)−Ni(1)−N(10)	89.38(13)	N(9)−Ni(1)−N(11)	89.98(13)

Table 3. Selected bond lengths and angles in complex **4**

Bond lengths (Å)			
Fe(1)−N(5)	1.970(2)	Fe(1)−N(7)	1.978(2)
Fe(1)−N(9)	1.973(3)	Fe(1)−C(10)	1.924(3)
Fe(1)−C(15)	1.939(3)	Fe(1)−C(16)	1.928(3)
C(15)−N(11)	1.147(4)	C(16)−N(12)	1.140(4)
C(10)−N(4)	1.153(4)	Cu(1)−N(4)	1.978(3)
Cu(1)−N(1)	1.996(3)	Cu(1)−N(2)	2.010(3)
Cu(1)−N(3)	1.994(3)	N(11)−Cu(1)#2	2.443(3)
Bond angles (°)			
Fe(1)−C(10)−N(4)	178.9(3)	Cu(1)−N(4)−C(10)	170.4(3)
Fe(1)−C(15)−N(11)	170.7(3)	Fe(1)−C(16)−N(12)	176.0(3)
C(15)−Fe(1)−C(16)	86.12(13)	C(15)−Fe(1)−C(10)	90.19(13)
N(4)−Cu(1)−N(2)	171.60(11)	N(1)−Cu(1)−N(4)	96.52(11)
N(1)−Cu(1)−N(3)	160.38(12)	N(2)−Cu(1)−N(3)	84.26(11)
N(4)−Cu(1)−N(11)#1[a]	103.60(11)	Cu(1)#2−N(11)−C(15)	138.1(3)

[a] #1: $x, -y + 1/2, z + 1/2$; #2: $x, -y + 1/2, z - 1/2$.

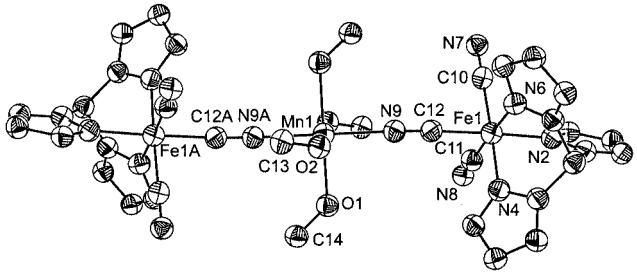

Figure 1. Molecular structure of $[(Tp)_2Fe^{III}{}_2(CN)_6Mn(CH_3OH)_4]\cdot 2CH_3OH$ (**2**); the solvate methanol molecules and hydrogen atoms have been omitted for clarity (ORTEP, 50% ellipsoids)

squashed octahedral geometry. Four oxygen atoms from the methanol molecules form the equatorial plane. The Mn(1)−O distances [2.198(2) and 2.1906(19) Å] are almost equivalent. Two cyanide nitrogen atoms occupy the axial positions. The Mn(1)−N(9) distance is 2.174(2) Å. The Mn(1)−N(9)≡C(12) bond angle [167.2(2)°] deviates significantly from 180°. The O(1)−Mn(1)−N(9) and O(2)−Mn(1)−N(9) bond angles are 89.72(9)° and 90.63(8)°, respectively. Non-coordinated CH_3OH molecules are inserted into the crystal spaces.

The intramolecular Fe···Mn and Fe···Fe separations are 5.193(2) and 10.386(3) Å, respectively, and the shortest intermolecular Fe···Fe, Mn···Fe, and Mn···Mn distances are 10.056(3), 8.819(5) and 10.950(3) Å, respectively.

The structure of complex **3** is very similar to that of complex **2** (Figure 2) except for the central $[Ni(cyclam)]^{2+}$ core. The Fe(1)−C(12)≡N(9) and Ni(1)−N(9)≡C(12) bond angles are 177.8(4)° and 171.5(3)°, respectively, which depart somewhat from strict linearity. The nickel atom is in an elongated octahedral environment. Four nitrogen atoms from the cyclam ligand form the equatorial plane. Two cyanide nitrogen atoms occupy the axial positions. The Ni(1)−N(9) distance is 2.096(3) Å, which is slightly longer than the average Ni−N(cyclam) bond length [2.061(3) Å].

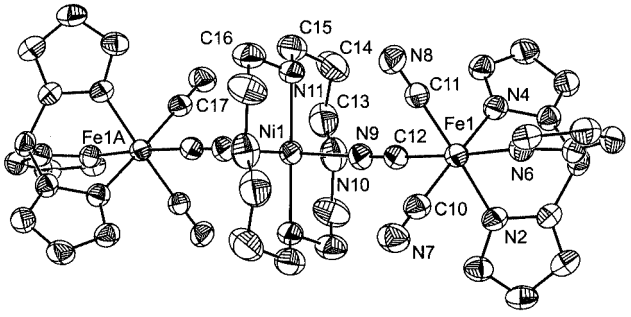

Figure 2. Molecular structure of $[(Tp)_2Fe^{III}{}_2(CN)_6Ni(cyclam)]\cdot 2H_2O$ (**3**); the solvate water molecules and hydrogen atoms have been omitted for clarity (ORTEP, 50% ellipsoids)

The intramolecular Fe···Ni and Fe···Fe separations through bridging cyanides are 5.132(2) and 10.265(5) Å, respectively. The shortest intermolecular Fe···Fe, Ni···Fe, and Ni···Ni distances are 7.622(4), 6.996(2) and 11.046(1) Å, respectively.

X-ray crystallography of **4** reveals that the structure consists of a one-dimensional cationic polymer $[\{TpFe(CN)_3\}\{Cu(dien)\}]_n^{n+}$, with free perchlorate counteranions (Figure 3 and 4). The zigzag chain is made up of a cyano-bridged alternating $[TpFe(CN)_3]^-$−$[Cu(dien)]^{2+}$ fragment. Within the chain, $[TpFe(CN)_3]^-$ uses two *cis*-CN groups to connect with two $[Cu(dien)]^{2+}$ units, while each $[Cu(dien)]^{2+}$ unit is linked to two $[TpFe(CN)_3]^-$ ions at *cis* positions. The central iron atom is six-coordinate with three Tp nitrogen atoms and three cyanide carbon atoms. The Fe(1)−N(Tp) bond lengths [1.970(2)−1.978(2) Å] are considerably shorter than those found in the high-spin iron(III) complex $[Fe(Tp)Cl_3]^-$ [2.152(4)−2.175(5) Å].[12] The Fe−C≡N angles of the bridging cyanide ligands [170.7(3)° and 178.9(3)°] and of the terminal cyanide groups [176.0(3)°] depart somewhat from strict linearity. The Cu^{II} center adopts a distorted square-pyramidal geometry, where one $[TpFe(CN)_3]^-$ unit is bound to the basal site [Cu(1)−N(4), 1.978(3) Å] and the other is bound to the elongated apical site [Cu(1)#2−N(11), 2.443(3) Å] [#2: x, $-y + 1/2$, $z - 1/2$]. The remaining three basal sites are occupied by the dien ligand, with an average Cu−N bond length of 2.000(3) Å. The value of the Cu(1)−N(4)≡C(10) bond angle is 170.4(3)°. However, the Cu(1)#2−N(11)≡C(15) bond angle is 138.1(3)°. The Fe···Cu separations within the chain are 5.040(2) Å for Fe(1)···Cu(1) and 5.062(2) Å for Fe(1)···Cu(1)#2. The shortest interchain Fe···Fe, Cu···Cu and Fe···Cu distances are 8.169(2), 13.345(2) and 11.062(4) Å, respectively.

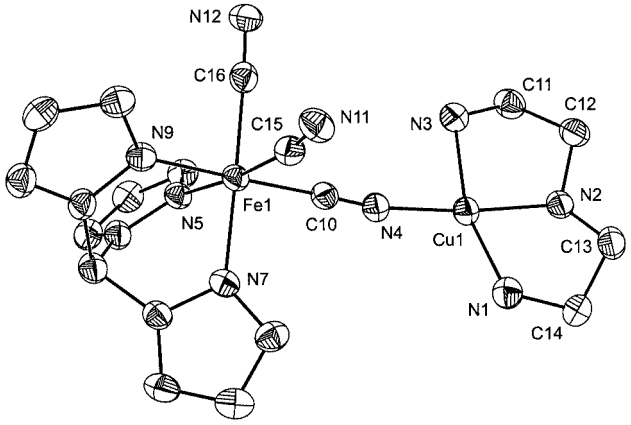

Figure 3. Molecular structure of $[(Tp)Fe^{III}(CN)_3Cu(dien)]ClO_4\cdot H_2O$ (**4**); the solvate water molecule, perchlorate and hydrogen atoms have been omitted for clarity (ORTEP, 50% ellipsoids)

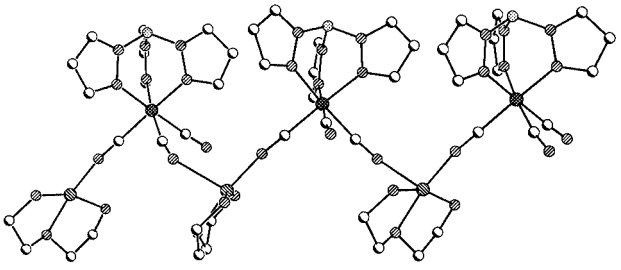

Figure 4. Structure of the one-dimensional chain of **4** running parallel to the *c* axis

Magnetic Properties

The temperature dependence of $\chi_M T$ for complex **2** (χ_M being the magnetic susceptibility per Fe_2Mn unit) is shown in Figure 5. The value of $\chi_M T$ at room temperature is 5.74 emu·K·mol^{-1} (6.78 μ_B). This value is consistent with the presence of a high-spin Mn^{II} atom and two low-spin Fe^{III} atoms magnetically isolated. As the temperature is lowered, $\chi_M T$ decreases steadily until it reaches a value of 1.03 emu·K·mol^{-1} at 2.0 K, indicating a weak antiferromagnetic interaction between the Mn^{II} and Fe^{III} ions.

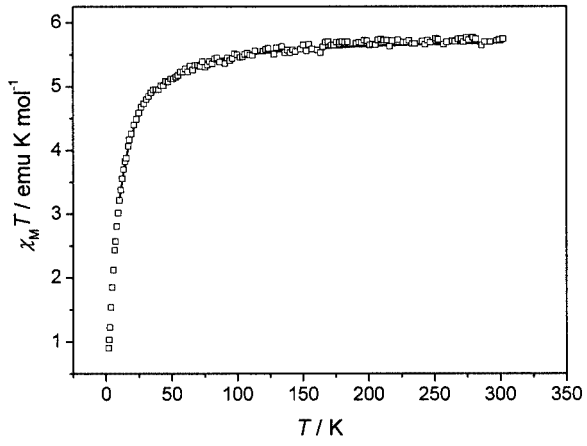

Figure 5. Plot of temperature dependence of $\chi_M T$ measured at 30 kOe field for **2**; the solid line represents the best-fit curve from 10 K to 300 K

The magnetic data has been fitted into the isotropic Hamiltonian:

$$\hat{H} = -2J\cdot(\hat{S}_1\cdot\hat{S}_2 + \hat{S}_2\cdot\hat{S}_3) - 2J'\cdot\hat{S}_1\cdot\hat{S}_3 \quad (1)$$

where $\hat{S}_1$, $\hat{S}_2$ and $\hat{S}_3$ are the spin operators of iron(III), manganese(II) and iron(III), respectively; J and J' are the intramolecular exchange coupling parameters between adjacent and peripheral spin carriers, respectively. Because the two iron(III) ions in the iron(III)-manganese(II)-iron(III) cluster are far apart, the quality of the fit does not depend on J', and hence the fit with $J' = 0$ has been used. The theoretical expression of the magnetic susceptibility of the Fe^{III}-Mn^{II}-Fe^{III} unit ($S_1 = S_3 = 1/2$, $S_2 = 5/2$) is:

$$\chi_M = Ng^2\beta^2/4kT(A/B) \quad (2)$$

where $A = 35 + 10\exp(-7J/kT) + 35\exp(-2J/kT) + 84\exp(5J/kT)$ and $B = 3 + 2\exp(-7J/kT) + 3\exp(-2J/kT) + 4\exp(5J/kT)$. The best fit to the experimental data above 10 K gives $J = -2.19$ cm^{-1} and $g = 2.13$. The agreement factor $R = \Sigma[(\chi_M T)_{obsd} - (\chi_M T)_{cald}]^2/\Sigma[(\chi_M T)_{obsd}]^2$ is 7.7×10^{-5}, which indicates a good agreement, as shown in Figure 5. The J value can be compared with the value of -0.9 cm^{-1} observed in another centrosymmetric Fe^{III}-Mn^{II}-Fe^{III} trinuclear complex.[9b]

The magnetic centers in complex **3** have similar linkages to complex **2**, but they show very different magnetic behaviors due to the replacement of the Mn^{II} ion in **2** by the Ni^{II} ion in **3** (Figure 6). For complex **3**, the value of $\chi_M T$ at room temperature is 2.70 emu·K·mol^{-1} (4.65 μ_B), which is higher than the expected spin-only value of 1.75 emu·K·mol^{-1} per Fe_2Ni unit ($g_{Fe} = g_{Ni} = 2$, $S_{Fe} = 1/2$ and $S_{Ni} = 1$), indicating a possible ferromagnetic coupling between the Fe^{III} and Ni^{II} centers. When the temperature is lowered, the $\chi_M T$ product increases up to a maximum value of 5.03 emu·K·mol^{-1} at 6.0 K and then decreases abruptly below this temperature. This indicates that the ferromagnetic interaction between the metal ions dominates the magnetic properties in this system, which is in agreement with the field dependence of the magnetization (the saturation magnetization $Ms = 4.65\ N\beta$, see Figure 7).

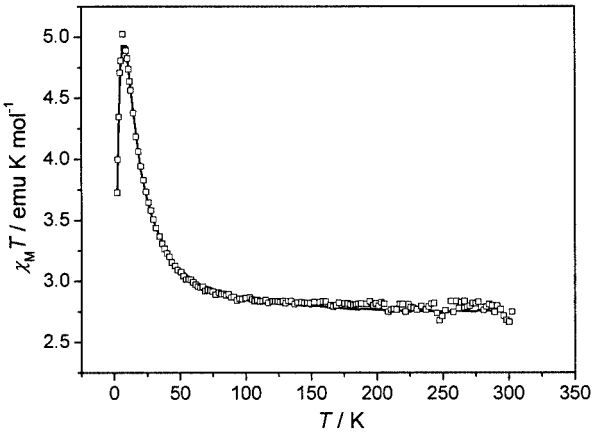

Figure 6. Plot of temperature dependence of $\chi_M T$ measured at 10 kOe field for **3**; the solid line represents the best-fit curve

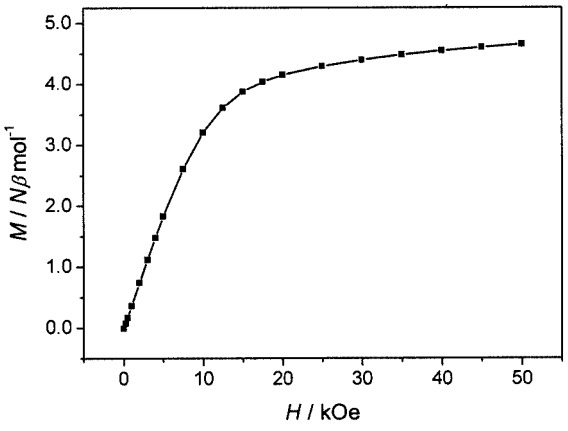

Figure 7. Field dependence of magnetization of complex **3** at 1.85 K

The same fitting method as complex **2** is suitable for the magnetic properties of complex **3**, except that $S_2 = 1$ (for Ni^{II} ion); the theoretical expression of the magnetic susceptibility is:

$$\chi_M = 2Ng^2\beta^2/kT(A/B) \quad (3)$$

where $A = 1 + 5\exp(2J/kT) + \exp(-2J/kT)$ and $B = 3 + 5\exp(2J/kT) + 3\exp(-2J/kT) + \exp(-4J/kT)$. The best fit to the experimental data in the whole temperature range gives $J = 17.2$ cm^{-1} and $g = 2.37$. The agreement factor $R = \Sigma[(\chi_M T)_{obsd} - (\chi_M T)_{cald}]^2/\Sigma[(\chi_M T)_{obsd}]^2$ is 9.2×10^{-4} (Figure 6).

The magnetic behavior of complex **4** (χ_M being the magnetic susceptibility per FeCu unit) is shown in Figure 8. $\chi_M T$ at room temperature is 1.21 emu·K·mol^{-1} (3.11 μ_B), a value expected for a low-spin iron(III) atom and a copper(II) atom magnetically isolated. It increases continuously on cooling, reaching a maximum value of 2.62 emu·K·mol^{-1} at 3 K, and then decreases to 2.33 emu·K·mol^{-1} at 2 K. This curve is in agreement with a ferromagnetic coupling between the Fe^{III} (S = 1/2) and Cu^{II} (S = 1/2) ions. The susceptibility data per FeCu (unit) can be fitted by a Curie−Weiss law $\chi_M = C/(T - \theta)$ in the temperature range 50−300 K, giving a Curie constant C of 1.20 emu·K·mol^{-1}, and a Weiss constant θ, of +6.16 K. The C value corresponds to one Fe^{III} (S = 1/2) ion and one Cu^{II} (S = 1/2) ion magnetically isolated. The positive value of θ indicates a ferromagnetic interaction between the Fe^{III} and Cu^{II} ions. On the basis of the crystal data, complex **4** has a 1-D zigzag chain structure and, furthermore, the Fe−CN−Cu linkages are unequal. Therefore, when the Heisenberg−Dirac−Van Vleck dimer model ($H = -2JS_1S_2$) or the 1-D uniform chain model[13] was used in this magnetic system, no rational result was obtained. To get a set of useful fitting results to interpret the magnetic exchange between the magnetic centers, the theoretical approach and treatment reported by Rojo and Kou[14] are suitable here. Thus, the 1-D chain can be considered as alternating uniform Fe−Cu dimers with different intradimeric and interdimeric exchange constants. Therefore,

$$\chi_d = \frac{2Ng^2\beta^2}{kT}\frac{1}{3+\exp(-2J_d/kT)} \quad (4)$$

$$\chi_d = \frac{Ng^2\beta^2}{3kT}S_d(S_d+1) \quad (5)$$

$$\chi_M = \chi_{chain} = \frac{Ng^2\beta^2}{3kT}\frac{1+u}{1-u}S_d(S_d+1) \quad (6)$$

where $u = \coth[J_cS_d(S_d + 1)/kT] - kT/[J_cS_d(S_d + 1)]$ and J_d and J_c are intradimeric and interdimeric exchange constants, respectively.

The best fit to the experimental data above 5 K gives J_d = 10.9 cm^{-1}, J_c = 1.29 cm^{-1} and g = 2.54. The agreement factor $R = \Sigma[(\chi_M T)_{obsd} - (\chi_M T)_{cald}]^2/\Sigma[(\chi_M T)_{obsd}]^2$ is 6.3 × 10^{-4} (Figure 8). The Fe^{III}-Cu^{II} exchange coupling parameter is comparable to that of the cyano-bridged cyclic tetranuclear complex $[Fe^{III}_2Cu^{II}_2(\mu\text{-}CN)_4(bipy)_6](PF_6)_6\cdot 4CH_3CN\cdot 2CHCl_3$ (J = 6.3 cm^{-1}).[9a] The small J_c value might be attributed to the more bent Cu(1)#2−N(11)≡C(15) bond angle [138.1(3)°], which has an unfavorable effect on the magnetic coupling.

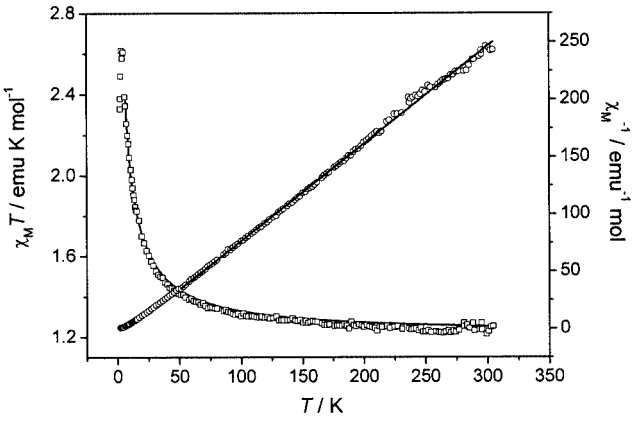

Figure 8. Plots of temperature dependence of $\chi_M T$ (open squares) and χ_M^{-1} (open circles) measured at 10 kOe field for **4**; the solid lines represent the best-fit curve from 5 K to 300 K for $\chi_M T$ and the best fit to the Curie−Weiss law from 50 K to 300 K for χ_M^{-1}

Experimental Section

Materials and Physical Measurements: $Ni(cyclam)(ClO_4)_2$ was synthesized as described previously.[15] The amine ligands diethylenetriamine (dien), 1,4,8,11-tetraazacyclotetradecane (cyclam) and all other reagents were purchased from standard sources and used as received. The IR spectra were recorded on a Nicolet-170SX FT-IR spectrophotometer with KBr pellets in the range 4000−400 cm^{-1}. Elemental analyses for C, H and N were performed on a Perkin-Elmer 240C analyzer. Variable-temperature magnetic susceptibility date were collected using a Quantum Design MPMS SQUID magnetometer. The experimental susceptibilities were corrected for the diamagnetism of the constituent atoms (Pascal's Tables).[16]

Safety Note: Although we have experienced no problem with the compounds reported in this work, perchlorate salts with organic ligands are often explosive and should be handled with great caution.

$[(Tp)_2Fe^{III}_2(CN)_6Mn(CH_3OH)_4]\cdot 2CH_3OH$ (2): Solid $Mn(ClO_4)_2\cdot 6H_2O$ (36 mg, 0.1 mmol) was added to a methanol solution (5 mL) of $(Bu_4N)[(Tp)Fe(CN)_3]$ (59 mg, 0.1 mmol). After slow evaporation of the resulting solution, red plate-like crystals **2** were formed and collected by filtration. Yield: 75%. $C_{28}H_{36}B_2Fe_2MnN_{18}O_4$: calcd. C 38.35, H 4.14, N 28.75; found C 38.61, H 4.45, N 28.64. IR (KBr): $\tilde{\nu}$ = 2129 (ν_{CN}) and 2151 cm^{-1} (ν_{CN}).

$[(Tp)_2Fe^{III}_2(CN)_6Ni(cyclam)]\cdot 2H_2O$ (3): A mixture of ethanol and water (1:1, 10 mL) was gently layered on top of a solution of $Ni(cyclam)(ClO_4)_2$ (91 mg, 0.2 mmol) in water (3 mL). A solution of $(Bu_4N)[(Tp)Fe(CN)_3]$ (118 mg, 0.2 mmol) in ethanol (2 mL) was added carefully as a third layer. Orange crystals of **3** were obtained after one week, washed with ethanol and diethyl ether, and dried in air. Yield: 60%. $C_{34}H_{46}B_2Fe_2N_{22}NiO$: calcd. C 42.06, H 4.78, N 31.74; found C 41.67, H 5.07, N 31.14. IR (KBr): $\tilde{\nu}$ = 2119 (ν_{CN}) and 2157 cm^{-1} (ν_{CN}).

$[(Tp)Fe^{III}(CN)_3Cu(dien)]ClO_4\cdot H_2O$ (4): A stock solution (0.075 M, 2 mL) of dien was added to an aqueous solution of

Table 4. Crystal and refinement data for complexes **2**−**4**

	2	**3**	**4**
Formula	$C_{30}H_{44}B_2Fe_2MnN_{18}O_6$	$C_{34}H_{46}B_2Fe_2N_{22}NiO$	$C_{16}H_{25}BClCuFeN_{12}O_5$
Formula mass	941.09	970.96	631.13
Crystal system	monoclinic	monoclinic	monoclinic
Space group	$P2_1/c$	$P2_1/c$	$P2_1/c$
a (Å)	9.3221(5)	9.6157(9)	13.902(2)
b (Å)	16.4877(9)	17.0115(15)	13.345(2)
c (Å)	14.4151(8)	14.0948(12)	15.007(2)
α (°)	90	90	90
β (°)	94.7070(10)	95.787(2)	112.978(3)
γ (°)	90	90	90
Z	2	2	4
V (Å^3)	2208.1(2)	2293.8(4)	2563.3(6)
D_{calcd} (g cm^{-3})	1.415	1.406	1.635
T (K)	213(2)	293(2)	213(2)
λ (Å)	0.71073	0.71073	0.71073
μ (mm^{-1})	0.990	1.085	1.553
F(000)	970	1004	1288
$2\theta_{max}$ (°)	50.0	52.0	52.0
hkl range	$-5 \le h \le 11$ $-19 \le k \le 18$ $-17 \le l \le 12$	$-11 \le h \le 7$ $-20 \le k \le 18$ $-16 \le l \le 17$	$-17 \le h \le 16$ $-15 \le k \le 16$ $-15 \le l \le 18$
Collected	8504	12217	15377
Unique	3816	4490	5037
Parameters	274	286	334
GOF	1.018	1.088	1.041
R_1 [$I > 2\sigma(I)$]	0.0440	0.0536	0.0478
wR_2 [$I > 2\sigma(I)$]	0.1138	0.1147	0.1198
(D map) max./min. [e·Å^{-3}]	0.202/−0.241	0.668/−0.350	0.442/−0.493

$Cu(ClO_4)_2 \cdot 6H_2O$ (4 mL, 56 mg, 0.15 mmol). A methanol solution of $(Bu_4N)[(Tp)Fe(CN)_3]$ (5 mL, 89 mg, 0.15 mmol) was added to this dark blue solution. Slow evaporation of the resulting solution in air afforded brown crystals. Yield: 80%. $C_{16}H_{25}BClCuFeN_{12}O_5$: calcd. C 30.45, H 3.99, N 26.63; found C 30.74, H 4.06, N 26.35. IR: (KBr): $\tilde{\nu}$ = 2131 (ν_{CN}) and 2157 cm^{-1} (ν_{CN}).

X-ray Crystallography: The structures of complexes **2**−**4** were determined. Suitable crystals were obtained by slow evaporation of the preparative reaction solution. Crystals were mounted in Paratone oil and placed in the dinitrogen cold stream of a Bruker Apex D8 diffractometer equipped with a 4 K CCD area detector for complex **2** or a Bruker-AXS P3 diffractometer equipped with a 1 K CCD area detector for complex **4**. Cell parameters were retrieved using SMART software and refined using SAINT on all observed reflections. Data were collected using the following strategy: 606 frames of 0.3° in ω with φ = 0°, 435 frames of 0.3° in ω with φ = 90°, and 235 frames of 0.3° in ω with φ = 180°. An additional 50 frames of 0.3° in ω with φ = 0° were collected to allow for decay correction. The highly redundant data sets were reduced using SAINT and corrected for Lorentz and polarization effects. Absorption corrections were applied using SADABS supplied by Bruker. Structures were solved by direct methods using the program SHELXL-97. The positions of metal atoms and their first coordination spheres were located from direct-methods *E*-maps; other non-hydrogen atoms were found in alternating difference Fourier syntheses and least-squares refinement cycles and, during the final cycles, refined anisotropically. Hydrogen atoms were placed in calculated positions and refined as riding atoms with a uniform value of U_{iso}. Crystallographic parameters and agreement factors are contained in Table 4.

CCDC-231294 (for **2**), -231295 (for **3**) and -231296 (for **4**) contain the supplementary crystallographic data for this paper. These data can be obtained free of charge at www.ccdc.cam.ac.uk/conts/retrieving.html or from the Cambridge Crystallographic Data Centre, 12 Union Road, Cambridge CB2 1EZ, UK [Fax: +44-1223-336033; E-mail: deposit@ccdc.cam.ac.uk].

Acknowledgments

This work was supported by The Major State Basic Research Development Program (G2000077500) and the National Natural Science Foundation of China (NSF20201006, 90101028, 20125104 and 20221101). The X-ray diffractometer is supported by NSF grant EAR-0003201.

[1] [1a] S. Ferlay, T. Mallah, R. Quahès, P. Veillet, M. Verdaguer, *Nature* **1995**, *378*, 701−703. [1b] S. M. Holmes, G. Girolami, *J. Am. Chem. Soc.* **1999**, *121*, 5593−5594.

[2] [2a] O. Sato, T. Iyoda, A. Fujishima, K. Hashimoto, *Science* **1996**, *271*, 49−51. [2b] N. Shimamoto, S. I. Ohkoshi, O. Sato, K. Hashimoto, *Inorg. Chem.* **2002**, *41*, 678−684. [2c] V. Escax, A. Bleuzen, C. Cartier dit Moulin, F. Villain, A. Goujon, F. Varret, M. Verdaguer, *J. Am. Chem. Soc.* **2001**, *123*, 12536−12543.

[3] [3a] C. P. Berlinguette, D. Vaughn, C. Canada-Vilalta, J. R. Galán-Mascarós, K. R. Dunbar, *Angew. Chem. Int. Ed.* **2003**, *42*, 1523−1526. [3b] V. Marvaud, C. Decroix, A. Scuiller, C. Guyard-Duhayon, J. Vaissermann, F. Gonnet, M. Verdaguer, *Chem. Eur. J.* **2003**, *9*, 1677−1691. [3c] V. Marvaud, C. Decroix, A. Scuiller, F. Tuyèras, C. Guyard-Duhayon, J. Vaissermann, J. Marrot, F. Gonnet, M. Verdaguer, *Chem. Eur. J.* **2003**, *9*, 1692−1705.

[4] [4a] K. R. Dunbar, R. A. Heintz, *Prog. Inorg. Chem.* **1997**, *45*, 283−391. [4b] M. Ohba, H. Ōkawa, *Coord. Chem. Rev.* **2000**, *198*, 313−328. [4c] H. Ōkawa, M. Ohba, *Bull. Chem. Soc. Jpn.* **2002**, *75*, 1191−1203. [4d] E. Coronado, F. Palacio, J. Veciana, *Angew. Chem. Int. Ed.* **2003**, *42*, 2570−2572.
[5] J. L. Heinrich, P. A. Berseth, J. R. Long, *Chem. Commun.* **1998**, 1231−1232.
[6] [6a] P. A. Berseth, J. J. Sokol, M. P. Shores, J. L. Heinrich, J. R. Long, *J. Am. Chem. Soc.* **2000**, *122*, 9655−9662. [6b] J. J. Sokol, M. P. Shores, J. R. Long, *Angew. Chem. Int. Ed.* **2001**, *40*, 236−239. [6c] M. P. Shores, J. J. Sokol, J. R. Long, *J. Am. Chem. Soc.* **2002**, *124*, 2279−2292.
[7] J. Y. Yang, M. P. Shores, J. J. Sokol, J. R. Long, *Inorg. Chem.* **2003**, *42*, 1403−1419.
[8] [8a] R. Lescouëzec, F. Lloret, M. Julve, J. Vaissermann, M. Verdaguer, R. Llusar, S. Uriel, *Inorg. Chem.* **2001**, *40*, 2065−2072. [8b] R. Lescouëzec, J. Vaissermann, C. Ruiz-Pérez, F. Lloret, R. Carrasco, M. Julve, M. Verdaguer, Y. Dromzee, D. Gatteschi, W. Wernsdorfer, *Angew. Chem. Int. Ed.* **2003**, *42*, 1483−1486.
[9] [9a] H. Oshio, O. Tamada, H. Onodera, T. Ito, T. Ikoma, S. Tero-Kubota, *Inorg. Chem.* **1999**, *38*, 5686−5689. [9b] R. Lescouëzec, F. Lloret, M. Julve, J. Vaissermann, M. Verdaguer, *Inorg. Chem.* **2002**, *41*, 818−826.
[10] R. Lescouëzec, J. Vaissermann, F. Lloret, M. Julve, M. Verdaguer, *Inorg. Chem.* **2002**, *41*, 5943−5945.
[11] [11a] Y. Zhang, J.-L. Zuo, H.-C. Zhou, R. H. Holm, *J. Am. Chem. Soc.* **2002**, *124*, 14292−14293. [11b] J.-L. Zuo, H.-C. Zhou, R. H. Holm, *Inorg. Chem.* **2003**, *42*, 4624−4631.
[12] H. Fukui, M. Ito, Y. Morooka, N. Kitajima, *Inorg. Chem.* **1990**, *29*, 2868−2870.
[13] J. C. Bonner, M. E. Fisher, *Phys. Rev. Sect. A* **1964**, *135*, 640−658.
[14] [14a] R. Cortés, M. Drillon, X. Solans, L. Lezama, T. Rojo, *Inorg. Chem.* **1997**, *36*, 677−683. [14b] H.-Z. Kou, B.-C. Zhou, D.-Z. Liao, R.-J. Wang, Y.-D. Li, *Inorg. Chem.* **2002**, *41*, 6887−6891.
[15] B. Bosnich, M. L. Tobe, G. A. Webb, *Inorg. Chem.* **1965**, *4*, 1109−1112.
[16] R. L. Carlin, *Magnetochemistry*, Springer-Verlag Publishers, Berlin, Heidelberg, **1986**.

Received February 14, 2004
Early View Article
Published Online July 6, 2004

